Supporting Information

Rapid Synthesis of Multifunctional β-cyclodextrin Nanospheres as Alkali-responsive Nanocarriers and Selective Antibiotic Adsorbents

Qiuju Li,[a,b] Dandan Wang,[a,b] Xian Fang,[a,b] Boyang Zong,[a,b] Ying Liu,[a,b] Zhuo Li,[a,b] Shun Mao[a,b,*] and Kostya (Ken) Ostrikov[c]

[a] Biomedical Multidisciplinary Innovation Research Institute, Shanghai East Hospital, State Key Laboratory of Pollution Control and Resource Reuse, College of Environmental Science and Engineering, Tongji University, 1239 Siping Road, Shanghai 200092, China

[b] Shanghai Institute of Pollution Control and Ecological Security, Shanghai 200092, China

[c] School of Chemistry and Physics and QUT Centre for Materials Science, Queensland University of Technology (QUT), Brisbane, QLD 4000, Australia

* Corresponding author. Tel.: +86-21-65982705

E-mail address: shunmao@tongji.edu.cn (S. Mao)

Experimental

1. Chemicals

Chemicals including β-cyclodextrin (98%), sodium periodate (AR), 2,4,6-triaminopyrimidine (TAP), 4,6-diamino -2-mercaptopyrimidine (DAMP, 95%) 1,1,1,3,3,3-hexafluoro-2-propanol (HFIP, 98%) were purchased from Aladdin Chemistry Co., Ltd (Shanghai, China). Ciprofloxacin (Cip, AR), ofloxacin (Ofl, AR), norfloxacin (Nor, AR), enoxacin (Eno, AR) and fleroxacin (Fle) were obtained from Sigma-Aldrich Ltd. (Shanghai, China). 4-amino-6-hydroxy-2-mercaptopyrimidine (AHMP, 98%) and 3-aminobenzeneboronic acid (APBA, 98%) were supplied by Shanghai Macklin Biochemical Co., Ltd. All chemicals and regents were used without further purification. Ultrapure water (18.2 MΩ·cm) produced from a Milli-Q system was used for all experiments.

2. Preparation of cyclodextrin-based nanospheres (CDNS)

β-cyclodextrin aldehyde (ACD) with high aqueous solubility was firstly obtained by modified periodate oxidation of β-cyclodextrin. 30 g β-cyclodextrin were dispersed in 200 mL, then 12 g sodium periodate were added. The above mixture was stirred for 3 hours under dark condition. After filtered with 0.22 μm membrane, ACD molecules were precipitated by adding 800 mL ethanol. The precipitates were washed with ethanol/water (80/20, V/V) for three times and dried in vacuum oven at 40°C.

CDNS were synthesized using a highly facile method as follows: 0.34 g ACD was dissolved in water (20 mL), followed by addition of 0.17 g AHMP. The mixture was

stirred for 5 min at 60 ℃ and the resultant suspension were collected and washed with water and ethanol for three times and dried in vacuum at 60 ℃. HB-CDNS were prepared as follows: the less-oxidated ACD (30 g) here were half-oxidized with 6.0 g sodium periodate. 0.051 g APBA was added to ACD solution (0.34 g in 20 mL) followed by addition of 0.17 g AHMP after 2 hours. The obtained products were washed and heated at 150 °C for 10 hours under N_2 atmosphere. The final products were collected for further use and characterization.

3. Drug loading and release under alkaline condition

The encapsulation of norfloxacin (Nor) into CDNS was carried out as follows: Nor (10, 15, 25 and 50 mg) was added to the ACD solution (20 mL, 17 mg/mL) and stirred for 30 minutes followed by addition of 0.17 g AHMP for cross-linkage and then incubated at room temperature for 24 h. To improve the solubility of Nor, 1,1,1,3,3,3-hexafluoro-2-propanol (HFIP, 1 mL) was added in synthetic system. The Nor-loaded CDNS was dialyzed against deionized water (200 mL) for 10 h to eliminate cytotoxic HFIP and residual Nor. Dialysate was collected and freeze-dried. The concentration of unloaded Nor was measured using a high-performance liquid chromatography (HPLC) instrument.

The pH-responsive release behavior of Nor-loaded CDNS was measured in PBS with different pH values (pH 4.0, 7.0, 7.6 and 7.8). Firstly, 10 mg Nor-loaded CDNS were dispersed in 200 mL of PBS solution at 37 °C. Then, an aliquot (1 mL) was withdrawn and filtered in syringes equipped with 0.2 μm PTFE filters after a certain

interval. The concentration of released Nor was measured with the above-mentioned HPLC instrument.

4. Antibiotics adsorption with HB-CDNS

Fluoroquinolone antibiotics adsorption removal experiments were performed at room temperature in water with a 300-rpm stirring rate. HB-CDNS were prepared into 50 mL (100 mg/L) solution and mixed with ciprofloxacin (Cip), ofloxacin (Ofl), norfloxacin (Nor), or enoxacin (Eno) (100 μg/L). The mixture was immediately stirred and 1 mL aliquots of the suspension were taken at certain intervals and filtered in syringes equipped with 0.22 μm PTFE filters. The residual concentration of the antibiotics in each sample was determined by HPLC instrument. Quantification of antibiotic concentrations was performed by HPLC (Agilent 1260) instrument equipped with Thermo Syncronics C18 column (250 mm × 4.6 mm, 5 μm) and UV detector. The concentrations of Cip, Eno, and Nor were measured at the wavelength of 278 nm. The concentrations of Fle and Ofl were measured at the wavelength of 286 nm and 293 nm, respectively. Methanol: water containing 0.1% phosphoric acid = 70:30 (v/v) was used as the mobile phase at a flow rate of 1.0 mL/min. The retension time of Cip, Eno, Nor, Fle, and Ofl is 7.115, 5.900, 7.224, 4.927, and 5.549 min, respetiviely. The calibriate curves are as follow： $y = 0.0668x - 0.0493$, $R^2 = 0.9997$ (Cip); $y = 0.0372x - 0.0205$, $R^2 = 1.0000$ (Eno); $y = 0.0338x - 0.1192$, $R^2 = 0.9992$ (Nor); $y = 0.0716x - 0.2603$, $R^2 = 0.9984$ (Fle); $y = 0.0745x - 0.1558$, $R^2 = 0.9895$ (Ofl).

5. Characterizations

Scanning electron microscope (SEM, Hitachi S-4800) and transmission electron microscope (TEM, A JOEL 2100F) was used to characterize the morphology of samples. Fourier transform infrared (FTIR) spectra were collected with a Nicolet 380 spectrometer (Thermo Electron Corporation, USA). X-ray photoelectron spectroscopy (XPS) spectra were obtained with Thermo ESCALAB 250XI Scanning X-ray Microprobe TM. X-ray diffraction (XRD) patterns were obtained on Bruker D8 Advance X-ray diffractometer. The micromeritics ASAP 2460 instrument was used to measure the Brunauer–Emmett–Teller (BET) surface area. Thermo-gravimetric (TGA) measurements were carried out by a Mettler TGA 2 analyzer in air atmosphere. Zetasizer Nano ZS 90 was used to determine zeta potential and hydrodynamic size of samples. The NMR spectra were recorded on a Bruker Avance III 400 MHz instrument at room temperature. Raman spectra (Horiba evolution) of the samples were recorded on a microscope using a laser excitation wavelength of 532 nm and collected over a spectral from 1600 to 50 cm^{-1}. The elemental analysis of CDNS was conducted on organic element analyzer (elementar vario micro cube).

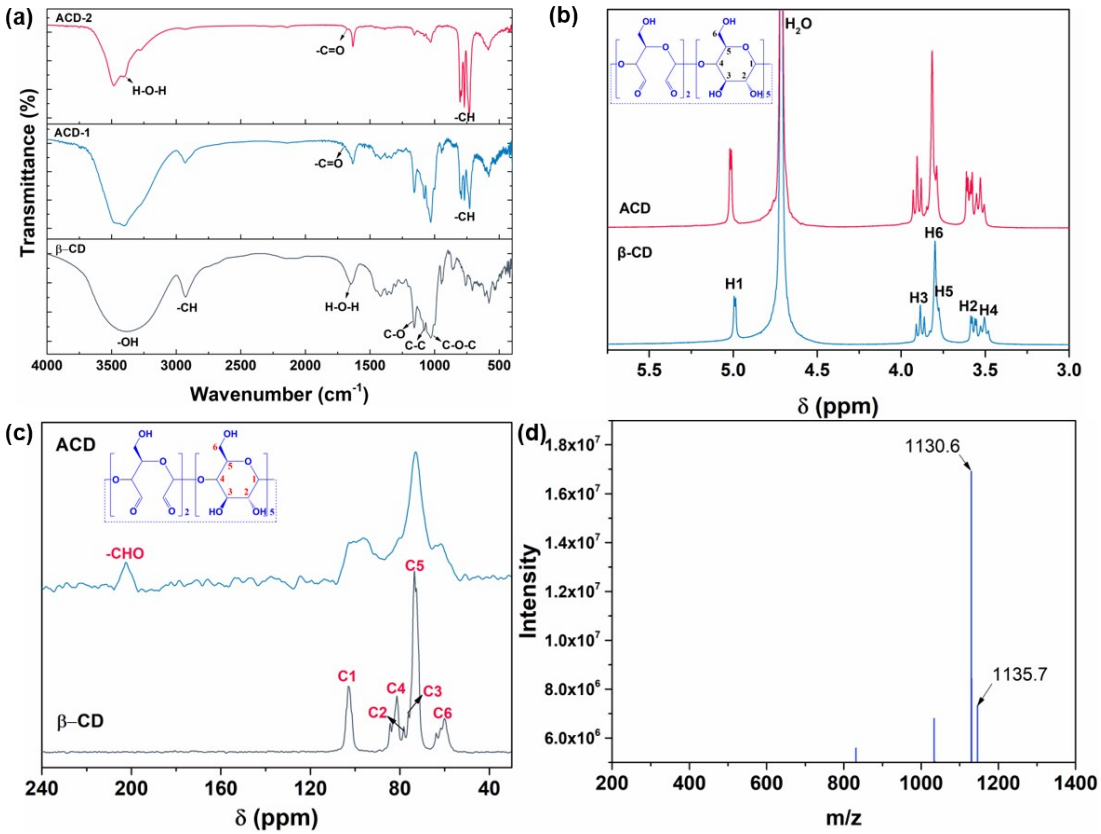

Fig. S1. (a) FTIR spectra of initial β-CD, ACD-1 (obtained with mole ratio of CD:$NaIO_4$ = 1:1), and ACD-2 (obtained with mole ratio of CD:$NaIO_4$ = 1:2). (b) ^1H NMR spectra of initial β-CD and aldehyde CD (ACD) in D_2O. (c) Solid state ^{13}C NMR spectra of initial β-CD and ACD. (d) MALDI-FT-IR MS spectra of ACD with 2,5-dihydroxybenzoic acid (DHB) as matrix material.

According to the FTIR spectra, after oxidation with $NaIO_4$, the peak at 1680 cm^{-1} for aldehyde group (-C=O) appears and increases with the increasing dosage of $NaIO_4$. The typical peaks for C-O-C glucosydic stretching vibration (1158 cm^{-1}), C-C stretching vibrations (1084 cm^{-1}), and C-O stretching vibrations (1028 cm^{-1}) are kept after oxidation with $NaIO_4$. More importantly, the peaks ranging from 950 to 530 cm^{-1} for

cyclodextrin ring indicate the complete structure reservation in ACD molecules[1, 2]. Besides, the peaks for O–H stretching vibration at 3386 cm^{-1} become sharper, mainly due to the cleavage of C-2, C-3-trans-diol position of D-glucose residues and thus the breakage of the hydrogen network[3]. The 1H NMR spectra of the pristine β-CD and ACD samples are shown in Fig. S1b. The typical peaks for H1 - H6 remain unchanged but show slight down-shifts. These results suggest that the porous structures of cyclodextrin remain in the oxidized ACD, which is consistent with the results of the previous studies[2]. Besides, based on the integral areas, the ratio of H2 and H3 integral area to the total H1-H6 integral area increases about 1.63% from initial β-CD to ACD, which means the degree of oxidation of cyclodextrin is about 8.73% (based on carbon atom). According to solid state ^{13}C NMR spectra, the peak for aldehyde groups is observed at 199.5 ppm, which further proves the selective oxidation of β-CD into aldehyde groups. Moreover, the matrix-assisted laser desorption/ionization (MALDI)-MS spectra show that the main ions at m/z of 1130.6 and 1135.7 correspond to protonated ACD and pristine β-CD, respectively, which is consistent with the proposed structure of ACD in Fig. 1.

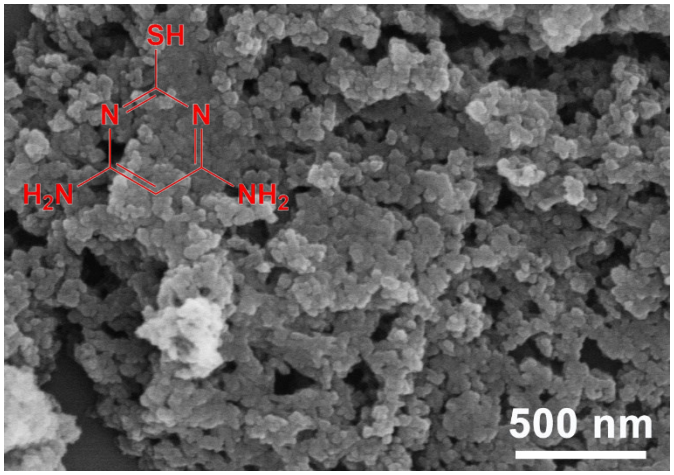

Fig. S2. SEM image of cyclodextrin-derived polymers with DAMP as cross-linkers.

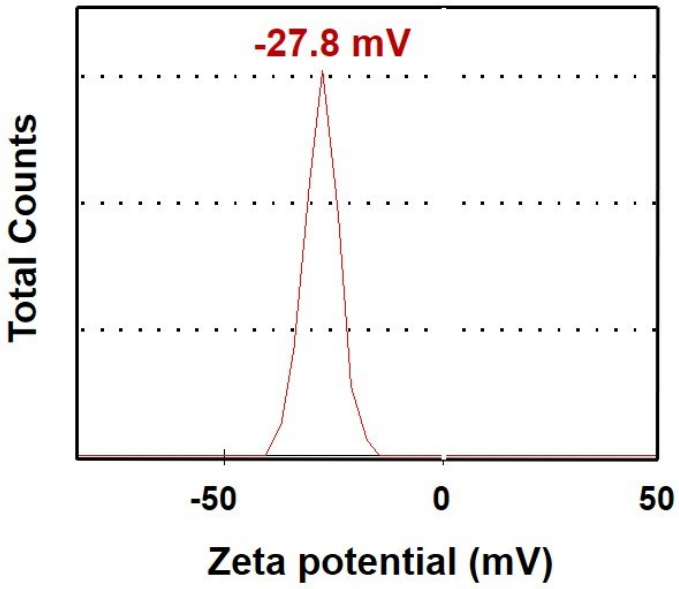

Fig. S3. Zeta potential of CDNS. The Zeta potential confirms the polymers after cross-linking are negatively charged. This may be attributed to the -OH and -COO groups.

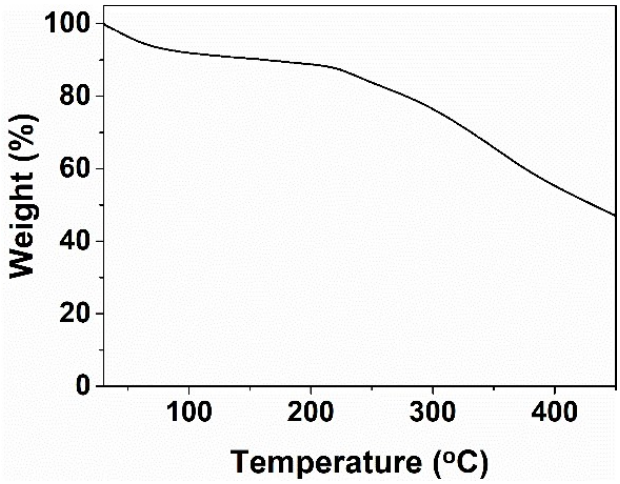

Fig. S4. TGA curve of CDNS.

Table S1 The element contents in CDNS.

Element	**C**	**H**	**O**	**N**	**S**
Content (wt.%)	29.7	4.3	21	25.7	19.3

According to the elemental analysis, the cyclodextrin moiety does not contain any N, S elements, whereas AHMP does. Therefore, the weight percentage of cyclodextrin is calculated as follow:

$$Weight\ ratio\ of\ \frac{ACD}{AHMP} = \frac{\frac{C_C\ in\ CDNS\ - C_N\ in\ CDNS/M_N\ in\ AHMP \times M_C\ in\ AHMP}{M_C\ in\ ACD}}{C_N\ in\ CDNS/M_N\ in\ AHMP},$$

$$Weight\ percentage\ of\ ACD\ in\ CDNS = \frac{Weight\ ratio\ of\ ACD/AHMP}{1 + Weight\ ratio\ of\ ACD/AHMP},$$

where $C_C\ in\ CDNS$ and $C_N\ in\ CDNS$ are the content of C and N element in the CDNS, respectively, while $M_N\ in\ AHMP$, $M_C\ in\ AHMP$, and $M_C\ in\ ACD$ are the weight percentage of N, C elements in AHMP and C element in ACD molecule, respectively. The calculated weight percentage of ACD in CDNS is about 35%, which indicates the

high density of cross-linking with AHMP as cross-linkers.

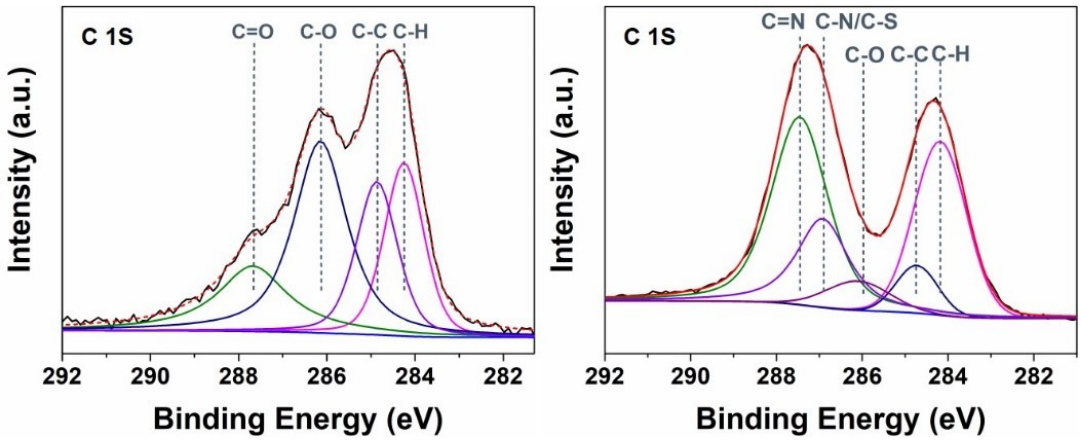

Fig. S5. The C1s XP spectra of ACD (left) and CDNS (right).

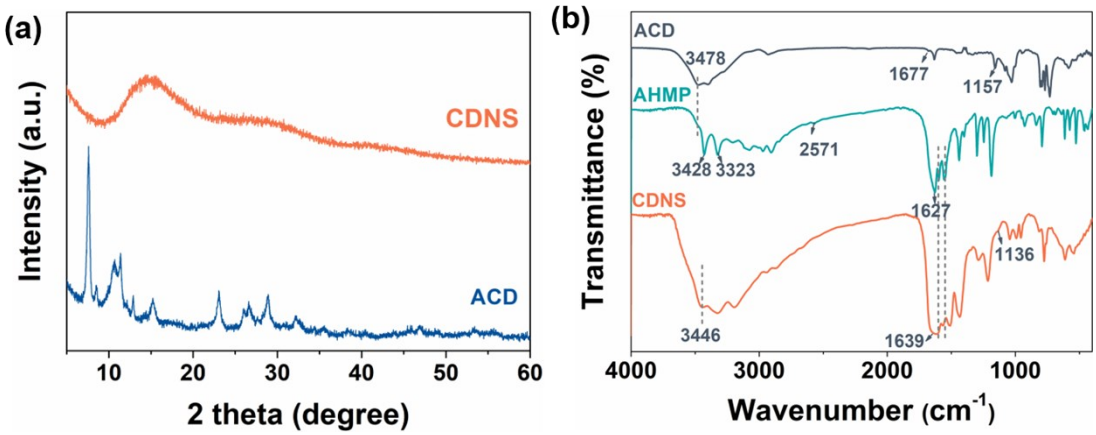

Fig. S6. (a) XRD patterns of ACD and CDNS. (b) FTIR spectra of ACD, AHMP and CDNS.

According to XRD patterns, compared with crystalline ACD, the broad peaks in the XRD pattern of CDNS confirmed the amorphous structure of the polymer network, in which the single cyclodextrin unities are randomly distributed without forming

crystalline domains. The XRD results match well with the HRTEM micrograph of CDNS in Fig. 1d, in which the amorphous structure of CDNS is clearly observed. Fig. S6b shows the FTIR spectra of ACD, AHMP and CDNS. After cross-linking with AHMP, the peak at 1677 cm^{-1} for the aldehyde symmetric vibration of ACD disappears, and the absorption peaks at 3428 cm^{-1} and 3323 cm^{-1} for $–NH_2$ stretching vibration of AHMP are significantly weakened due to the formation of C=N bonds. The broad peak centred at 1639 cm^{-1} appears due to the absorption of the C=N stretching vibration.

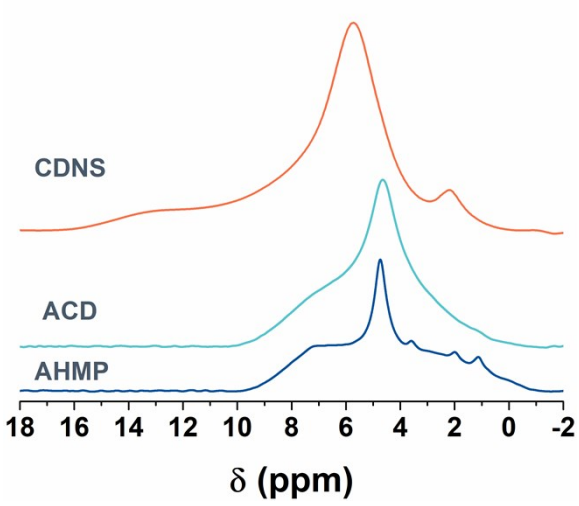

Fig. S7. The solid ^1H NMR spectra of AHMP, ACD, and CDNS.

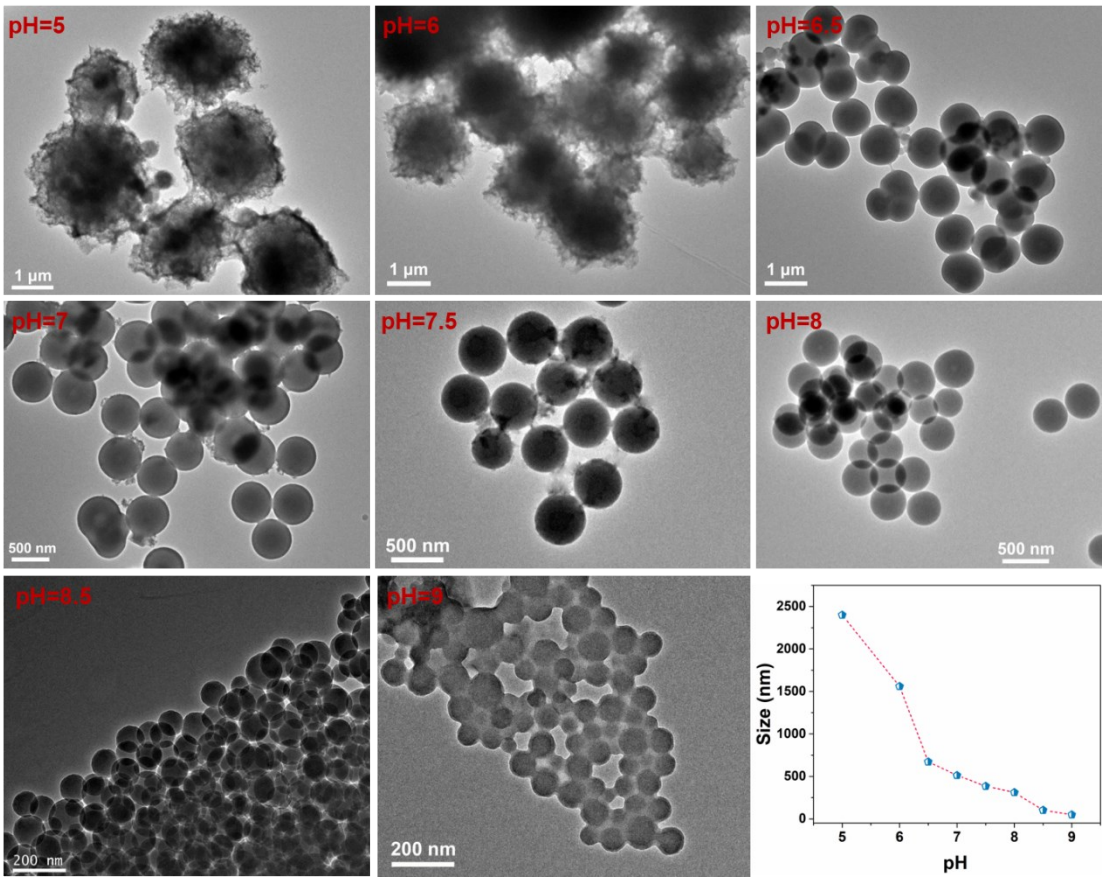

Fig. S8 TEM images of products obtained at different pH values. The size of the obtained spheres decreased with increasing pH from 5.0 to 9.0.

The TEM images in Fig. S8 show the irregular microspheres with diameter of 2.4 μm (pH 5.0) and 1.5 μm (pH 6.0) formed in the acidic media. When increasing the pH of reaction media from 7.0 to 9.0, the size of obtained sample decreased from 510 nm to 50 nm. When the pH value of reaction media is above 9.0, the cross-linking reaction cannot happen.

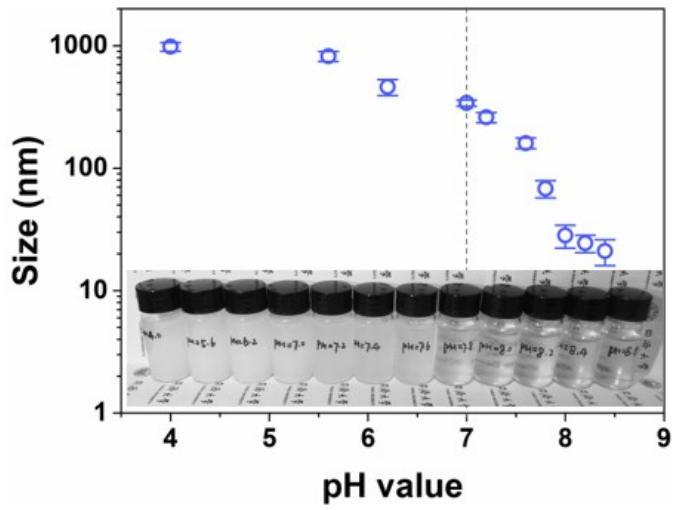

Fig. S9. Hydrodynamic size changes of CDNS in PBS solution with different pH values (1 mg/mL CDNS in PBS solution) (inset: the photos of CDNS suspension with different pH values).

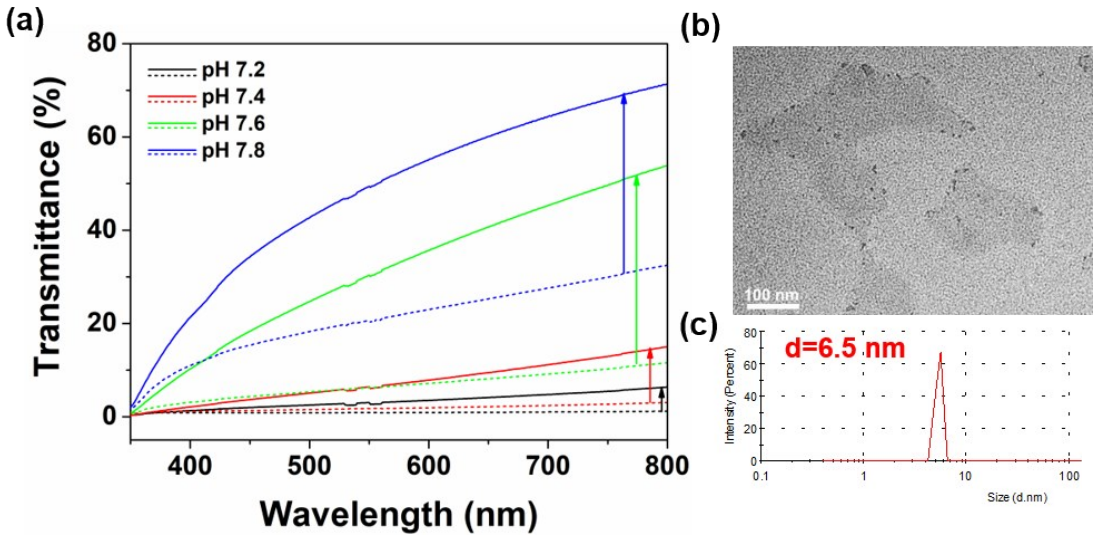

Fig. S10. (a) Transmittance curves of CDNS dispersion at high pH (7.2-7.8) for 30 min (dash line) and 120 min (solid line). (b) TEM image and (c) hydrodynamic size of resultant samples of CDNS treated at pH 7.8 with prolonged time of 120 min.

To investigate the stability of resultant sample obtained at high pH values, we

tested the transmittances of CDNS dispersion at pH 7.2-7.8 for 30 min and 120 min. The results in Fig. S10a show that the ongoing disassembly of CDNS leads to higher transmittance at prolonged time. Compared with the product size after 30 min disassembly (Fig.3b), the TEM image in Fig. S10b shows a decreased size of ~5 nm after 120 min, which is also confirmed by the dynamic light scattering measure (the hydrodynamic size of nanoparticle is about 6.5 nm). The above results indicate the instability of CDNS at high pH and gradual disassembly of cyclodextrin-based polymer into nano-scale cracks.

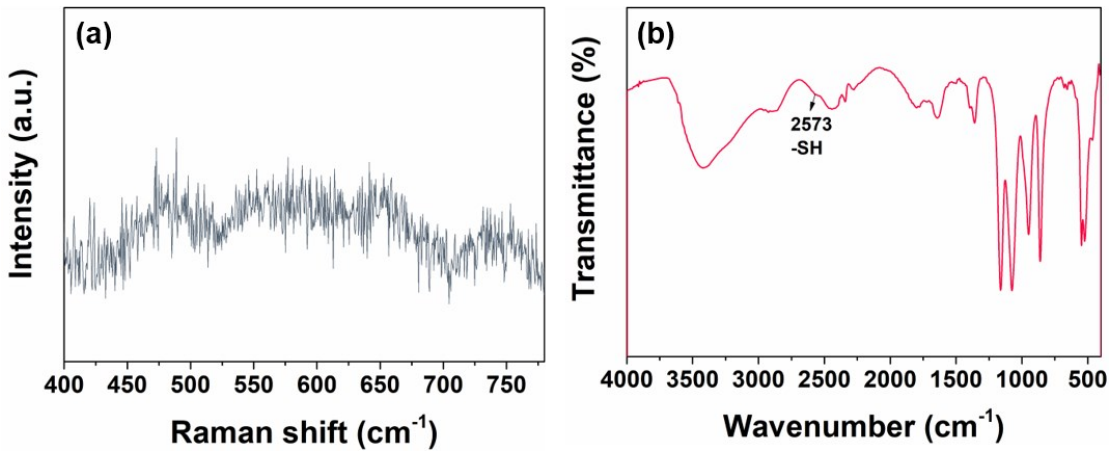

Fig. S11. (a) Raman and (b) FTIR spectra of residue CDNS at pH 7.8.

The residue samples of CDNS treated with PBS solution at pH 7.8 were collected and tested with Raman and FTIR spectroscopy. As shown in Fig.S11, the peaks located at 480-540 cm^{-1} (S-S groups) disappeared due to the cleavage of disulfide bond due to nucleophilic attack of OH^- ions. The FTIR spectrum in Fig. S11b shows the typical peak for -SH at 2573 cm^{-1}, which verifies the S-S bond scission into -SH groups.

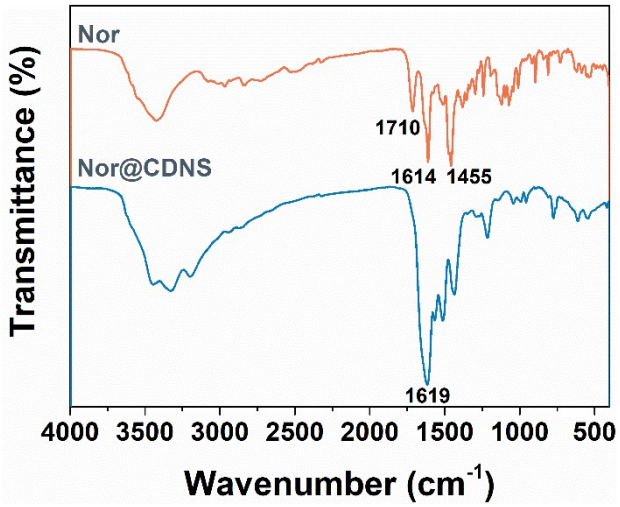

Fig. S12. FTIR spectra of Nor and Nor@CDNS.

For the FTIR spectrum of Nor, the peak at 1614 cm^{-1} and 1455 cm^{-1} originates from N-H bending vibration in quinolones structure and stretching vibration of O-C-O group, respectively. The peak at 1710 cm^{-1} in Nor is attributed to C=O stretching vibration in COOH groups. There were obvious changes in the spectrum of Nor@CDNS compared with that of Nor, in which the peak of COOH disappears, suggesting this functional group is embedded within the cavity of β-CD[4]. Meanwhile, due to the loading of Nor, the peak at 1639 cm^{-1} (C=N stretching vibration in CDNS) blueshifts to 1619 cm^{-1}. The above results thus confirm the successful encapsulation of Nor into CDNS.

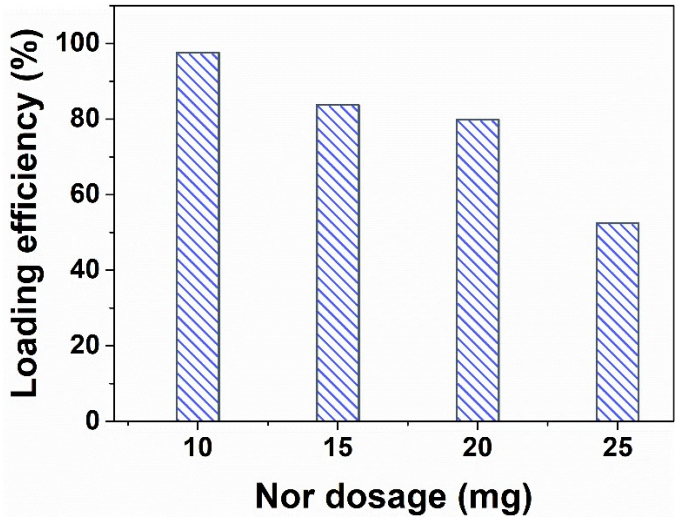

Fig. S13. Preloading efficiency of Nor with different dosages.

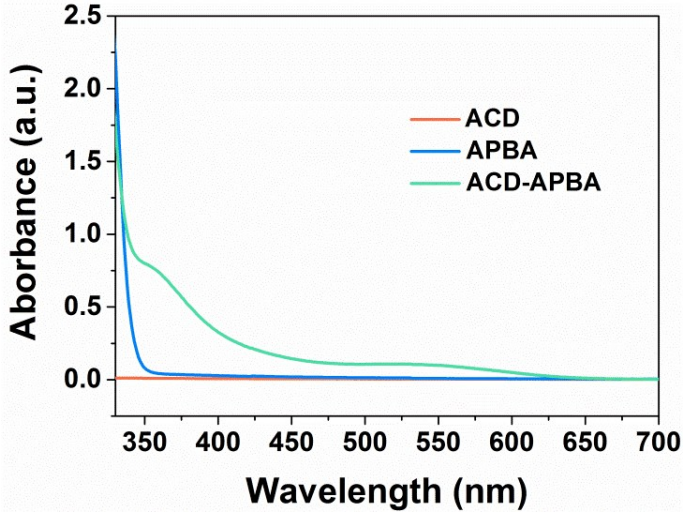

Fig. S14. UV/Vis absorption spectra of ACD, APBA, and ACD-APBA. The new peak at 520 nm is attributed to the formation of boronate esters. Another new peak at 355 nm is attributed to the formation of C=N bonds.

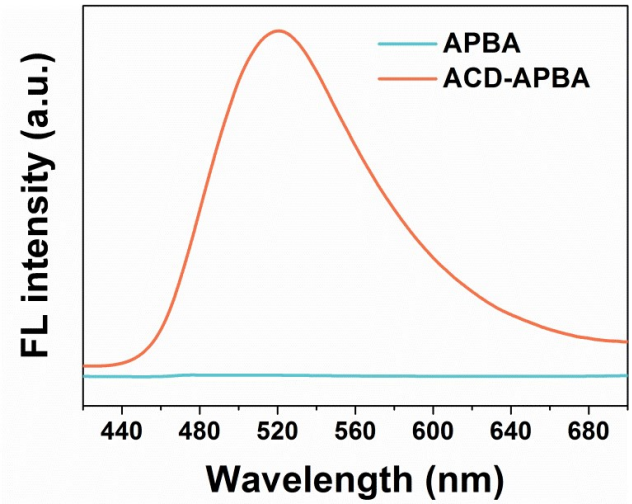

Fig. S15. FL spectrum of APBA and ACD-APBA. The fluorescence peak centered at 518 nm belongs to the n-π* transition from Schiff-base bond due to reaction between ACD and APBA.

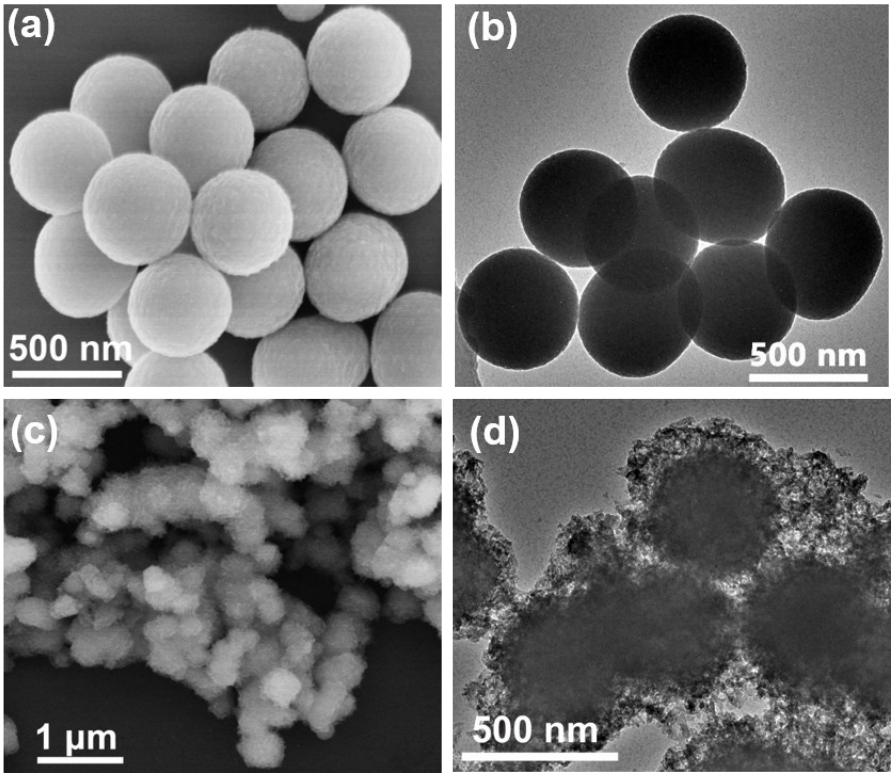

Fig. S16. SEM images of (a, b) B-CDNS and (c) HB-CDNS. (d) TEM image of HB-CDNS.

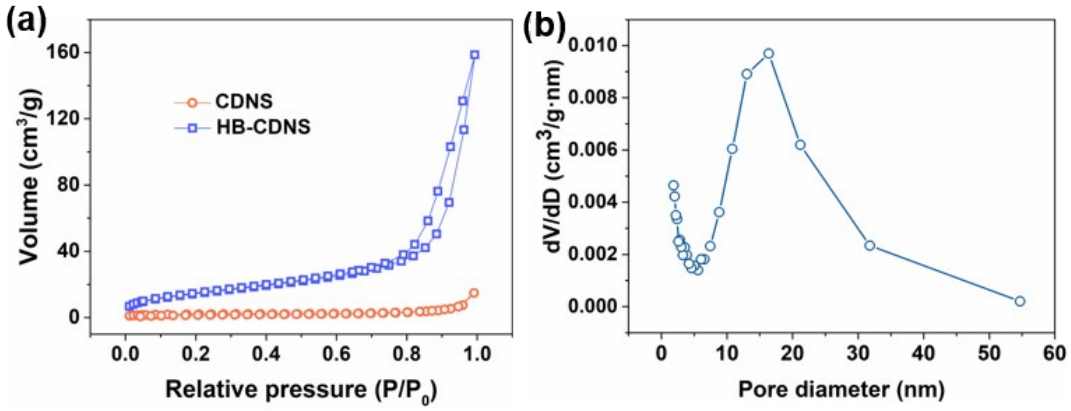

Fig. 17. (a) N_2 adsorption patterns of CDNS and HB-CDNS. (b) Pore distribution of HB-CDNS.

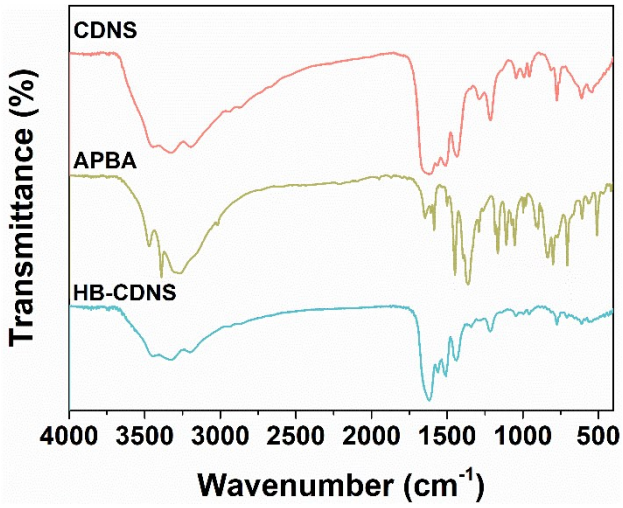

Fig. S18. FTIR spectra of CDNS, APBA, and HB-CDNS.

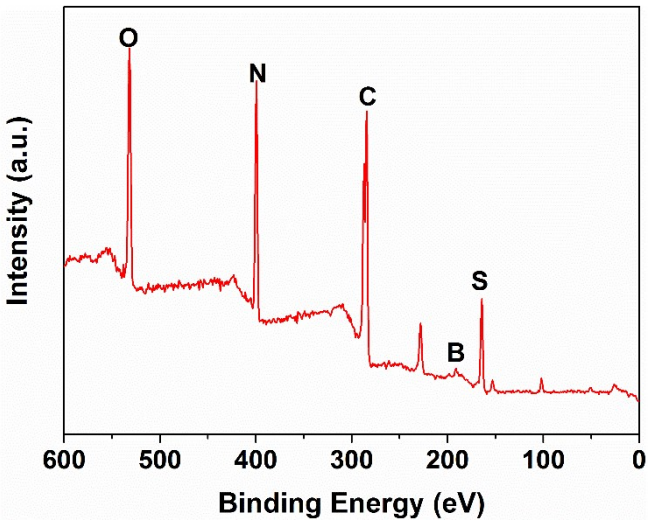

Fig. S19. XPS survey spectrum of HB-CDNS.

Table S2 Elemental contents of samples from XPS results.

Elements	CDNS	B-CDNS	HB-CDNS
C	48.3	46.2	46.6
O	17.9	12.7	13.7
N	26.6	26.7	27.2
S	7.2	6.7	6.9
B	/	7.7	5.6

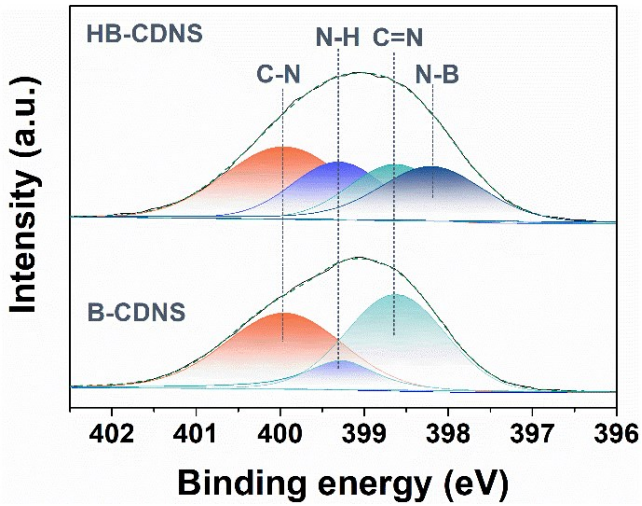

Fig. S20. N 1S high–resolution XP spectra of B-CDNS and HB-CDNS samples.

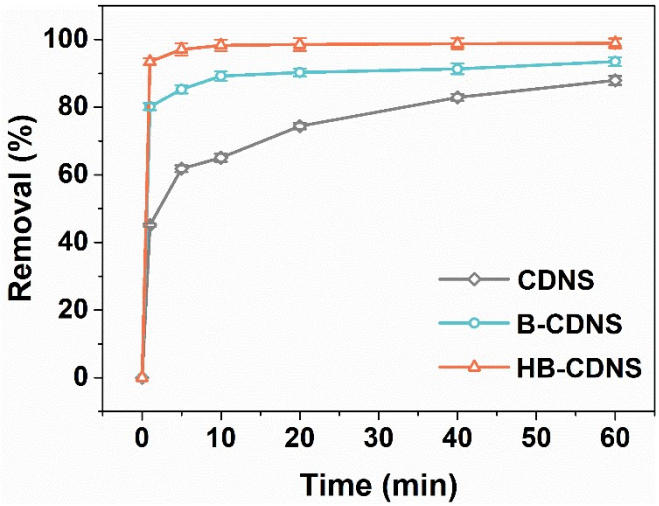

Fig. S21. Adsorption removal of Eno with CDNS, B-CDNS, and HB-CDNS samples.

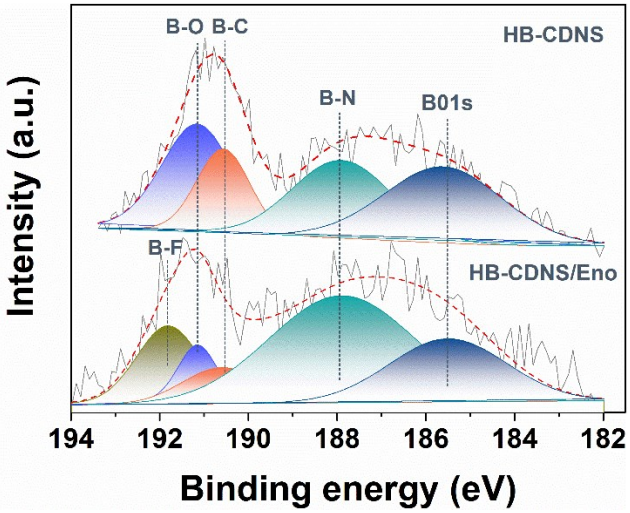

Fig. S22. B 1S high–resolution XP spectra of HB-CDNS and Eno-adsorbed HB-CDNS.

References

1. X. Ge, J. He, F. Qi, Y. Yang, Z. Huang, R. Lu and L. Huang, Spectrochim. Acta A, 2011, 81, 397-403.

2. C. Lou, X. Tian, H. Deng, Y. Wang and X. Jiang, Carbohyd. Polym., 2020, 231, 115678.

3. M. Kobayashi, T. Urayama, I. Suzawa, S. Takagi, K. Matsuda and E. Ichishima, Agricultural and Biological Chemistry, 1988, 52, 2695-2702.

4. G. O. K. Loh, Y. T. F. Tan and K. K. Peh, Carbohyd. Polym., 2014, 101, 505-510.